



Merger and non-merger galaxy clusters in cosmological AMR simulations.

Vazza F.^{1,2}¹ Jacobs University Bremen, Campus Ring 1, 28759, Bremen, Germany² INAF/Istituto di Radioastronomia, via Gobetti 101, I-40129 Bologna

Abstract. *Aims:* We discuss the dependence of shocks, cosmic rays acceleration and turbulence on the dynamical state of the host clusters. *Method:* We perform cosmological simulations with the grid code ENZO 1.5, with a mesh refinement scheme tailored to follow at high resolution shocks and turbulence developed in the clusters volume. *Results:* Sizable differences are found when some important properties, connected to non-thermal activity in clusters, are compared for post-merger, merging and relaxing systems.

Key words. galaxy: clusters, general – methods: numerical – intergalactic medium

1. Introduction

Numerical simulations presently provide a unique way to study the generation and evolution of shock waves, turbulence and chaotic motions following the evolution of large scale cosmic structure over a wide range of scales, and in a fully-time dependent way (Dolag et al. 2008 and references therein). Simulations can also be a very powerful approach to tackle the problem of explaining the occurrence and morphologies of non-thermal emissions in clusters, observed in many systems (e.g. Ferrari et al. 2008 for a review). We recently employed a tailored Adaptive Mesh Refinement (AMR) scheme in the ENZO cosmological code (e.g. O’Shea et al. 2004; Norman et al. 2007) in order to study these phenomena with unprecedented high dynamic range (Vazza et al. 2010a; Vazza et al. 2010d). Here we summarize some of the most important findings of our

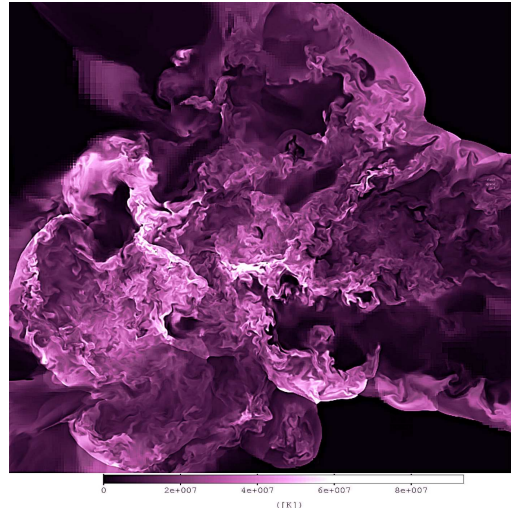


Fig. 1. Map of gas temperature for a major merger at $z \approx 0.6$. The side of the image is 8.8 Mpc/h, the depth along the line of sight is 25kpc/h.

Send offprint requests to: e-mail:
f.vazza@jacobs-university.de

work, reporting dependences between shocks, CR acceleration and turbulence and the dynamical state of the simulated host clusters.

2. ENZO Simulations.

The computations presented in this work were performed using the ENZO 1.5 code developed by the Laboratory for Computational Astrophysics at the University of California in San Diego (<http://lca.ucsd.edu>), see also O’Shea et al. (2004) and Norman et al. (2007).

We performed non-radiative Λ CDM simulations sampling a total cosmological volume with the size of $L_{\text{box}} \approx 440 \text{ Mpc}/h$, in which we re-simulated the evolution of the 20 most massive galaxy clusters, with a DM mass resolution of $m_{\text{DM}} = 6.76 \cdot 10^8 M_{\odot}$ and a peak spatial resolution of $\Delta x \approx 25 \text{ kpc}/h$ inside $< 3R_{\text{vir}}$ for each cluster (Vazza et al. 2010a). Our Adaptive Mesh Refinement (AMR) strategy was tailored to keep the maximum available resolution also at large distances from the cluster centers, tracking the propagation of strong discontinuities in the velocity field associated with shocks or turbulent motions (see Vazza et al. 2009b for a detailed discussion). At $z = 0$ each simulated clusters is sampled with a high number of cells, $N_{\text{grid}} \sim 500^3 - 600^3$, allowing a study of the intra cluster medium (ICM) across 2-3 orders of magnitude in spatial scales (see Fig. 1 for a representative example).

Our clusters have total masses in the range $6 \cdot 10^{14} \leq M/M_{\odot} \leq 3 \cdot 10^{15}$; they were divided according to their dynamical state, following in detail their matter accretion history for $z < 1.0$ (see Vazza et al. 2010a for details). According to this definition, our sample contains 10 post-merger systems (i.e. clusters with a merger with a mass ratio larger than 1/3 for $z \leq 1$), 6 merging clusters and 4 relaxed clusters at $z = 0$.

3. RESULTS

3.1. Shocks and Cosmic Rays

We identified shocks in the ICM with the same procedure presented in Vazza et al. (2009a), based on the analysis of velocity jumps across

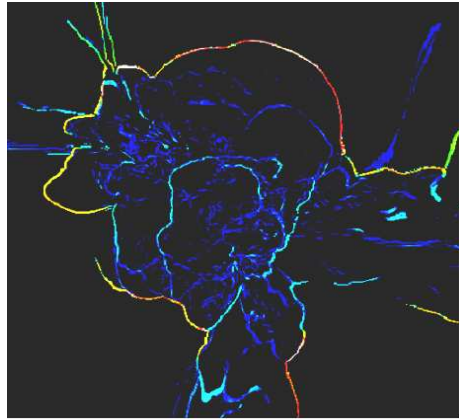


Fig. 2. 2-dimensional slice showing the Mach number of shocks for cluster E1 of our sample. The side of the slice is 13 Mpc/h and the depth along the line of sight is 25 kpc/h.

close cells (see Figure 2 for a map of the reconstructed Mach numbers). All clusters show similar shocks frequencies and energy distribution inside R_{vir} : the profiles of average Mach numbers are very flat and characterized by very weak shocks, $M < 2$ (top panel of Fig.3). *Sizable and stronger shocks ($M \sim 2.5 - 3.5$) are detected only in one post-merger systems and in one merging system.* The volume distribution of shocks is very steep ($\alpha \leq -4$ with $\alpha = d \log N(M)/d \log M$), while the distribution of flux of thermal energy through shock surfaces shows a well defined peak of thermalization at $M \sim 2$ (see bottom panel of Fig.3). In general our distributions are slightly steeper than what was previously reported in the literature (e.g. Ryu et al. 2003; Pfrommer et al. 2006; Skillman et al. 2008), which can be explained as an effect of different resolution, re-ionization models and shocks detection schemes. Only for the few $M > 2$ cases reported above the flux distribution is flatter, with $\alpha \sim -2$. We investigated the injection of relativistic protons (CR) at shocks applying the efficiency function introduced by Kang & Jones (2007) in the framework of the Diffusive Shock Acceleration model. We found that the ratio between the CR energy flux and the thermal flux is < 0.05 inside $0.2R_{\text{vir}}$ and

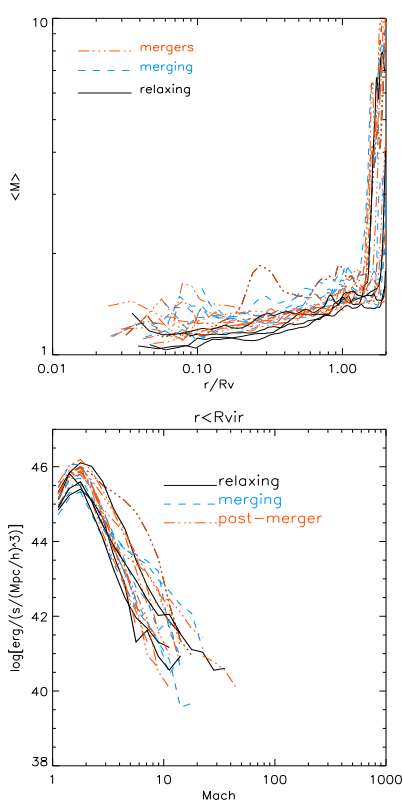


Fig. 3. Top: radial profile of average Mach number for the shocks in our sample. Bottom: distribution of thermal energy flux at shocks in the cluster samples.

< 0.1 inside R_{vir} . Only in one strong post-merger system we measure a CR injection of $\sim 0.2 - 0.3$ of the thermal energy flux. The estimated amount of CR energy inside clusters implied by our results is well below ~ 0.1 , which is presently allowed by observational upper limits coming from the non detection of gamma radiation from secondaries (e.g. Aleksic et al. 2010) and from the non detection of diffuse radio emission in relaxed clusters (Brunetti et al. 2007).

3.2. Turbulence

The turbulence in the ICM is expected to be sustained by the hierarchical process of mat-

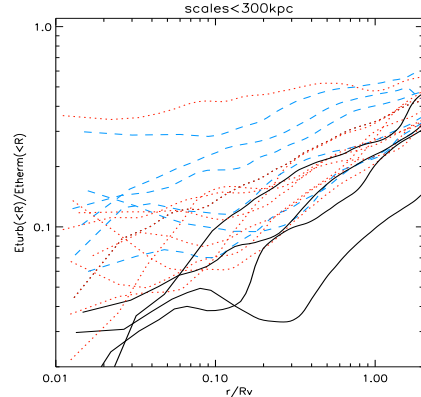


Fig. 4. Radial profile of the ratio between turbulent energy inside a given radius, and the thermal energy. The colors are as in Fig.3.

ter accretion in evolving galaxy clusters (e.g. Norman & Bryan 1999; Dolag et al. 2005; Iapichino & Niemeyer 2008). In Vazza et al. (2010d) we discussed the application of 2 different filtering techniques to disentangle the local mean velocity field of the gas (assuming it is laminar above a certain scale) and the turbulent velocity field. Despite small differences from case to case, the two methods provided consistent estimates of the turbulent energies of our clusters (see Sec.3.1 of Vazza et al. 2010d). In Fig.4 we show the radial profile of the turbulent to thermal energy ratio (for the filtering at the scale of ≈ 300 kpc) for all clusters in our sample. As expected turbulent motions are strong in merging and in post-merger systems ($E_{\text{turb}}/E_{\text{therm}} \sim 0.1 - 0.3$ for $r < 0.2R_{\text{vir}}$), while they are rather weak within the cores of relaxed systems ($E_{\text{turb}}/E_{\text{therm}} < 0.05$). However, almost all clusters host a sizable amount of turbulence ($\sim 20 - 40 E_{\text{therm}}$) within the total virial volume. An interesting finding of our simulations is that, on average, the turbulent energy present in merging systems is slightly larger than the turbulent energy of post-merger systems, when normalized to the thermal energy of the host cluster. This happens because the thermal energy inside the two clusters is initially lowered as an effect of the accretion of cold gas from filaments, while the turbulent energy almost steadily in-

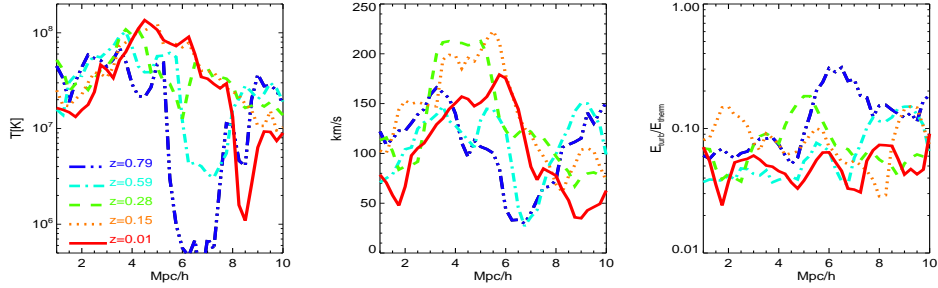


Fig. 5. Evolution of the profiles of gas temperature, turbulent gas velocity and $E_{\text{turb}}/E_{\text{therm}}$ along the axis of merger of two colliding clusters.

creases (see panels of Fig.5 and also the discussion in Sec.3.2 of Vazza et al. 2010d). Our sample is large enough to allow the statistical study of the occurrence of turbulence in cluster cores, and to compare with some basic expectation from the theoretical "turbulent re-acceleration" (e.g. Brunetti et al. 2001), as for instance with the estimated frequency of "turbulent" clusters. We investigated this issue in detail, by considering the typical volumes and turbulent energies needed to produce realistic radio halo emission: at $z \sim 0$, about 1/3 of our simulated clusters host a level of turbulent energy of $\sim 0.25E_{\text{therm}}$ inside a volume of $\sim R_{\text{vir}}/3$, in line with existing observations (Fig.6). Despite these rather large values of turbulence in merging or post-merger clusters, the ICM at the smallest scale is only weakly turbulent, as follows from the general shape of the velocity power spectrum of our simulated ICM (Vazza et al. 2010c; Xu et al. 2009). If turbulence in our clusters is computed for the typical spatial scales of real X-ray observations performed with XMM-Newton (e.g. Sanders et al. 2010), ~ 30 kpc, the simulated turbulent velocities of the ICM within the core region of clusters are much smaller than the upper limits from observations (see Fig.7).

3.3. Azimuthal Scatter of Gas Profiles

We investigated the level of intrinsic azimuthal scatter from the center of our clusters, focusing on some important thermodynamical

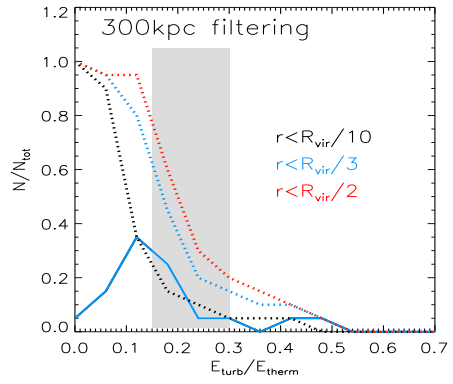


Fig. 6. Cumulative distribution function for $E_{\text{turb}}/E_{\text{therm}}$ inside $R_{\text{vir}}/2$, $R_{\text{vir}}/3$ and $R_{\text{vir}}/10$ for the simulated clusters assuming $l < 300\text{kpc}$ for turbulence. The solid line shows the differential distributions for $R_{\text{vir}}/3$. The grey band shows the turbulence required in the turbulent re-acceleration scenario (e.g. Brunetti & Lazarian 2010).

quantities (e.g. density, temperature, entropy and X-ray luminosity). This is interesting because recent long SUZAKU exposures measured sizable differences between the cluster profiles in different sectors from the center (e.g. Bautz et al. 2009; George et al. 2009). The inspection of the radial properties of our simulated data offers a way to assess the need of non-gravitational physics in simulations, such as AGN, Cosmic Rays, magnetic field, in

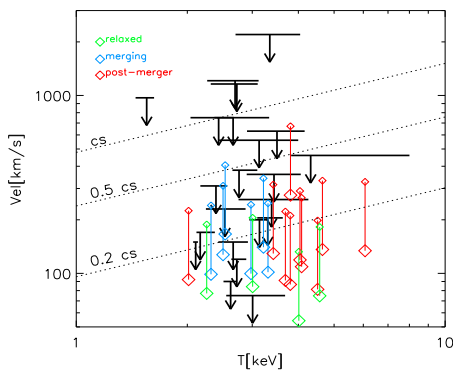


Fig. 7. Relation between temperature and turbulent velocity dispersion (small squares) for our clusters (squares in colors) and for the XMM-Newton observations of Sanders et al. (2010). The thick squares are for turbulent field below $< 30\text{kpc}$.

order to reconcile with observations. In Vazza et al. (2010 c) we tackled this issue by analyzing ENZO and GADGET2 runs of comparable resolution (Dolag et al. 2005). We processed all clusters with the filtering technique introduced in Roncarelli et al. (2006), designed to remove the densest clumpy gas component from each cluster dataset, and computed the cluster profiles in sectors of different angular size. In Fig.8 we report the azimuthal scatter ($\Delta\alpha = \pi/8$) for the different quantities in the ENZO clusters. *Post-merger clusters present the largest degree of azimuthal scatter at all radii while the relaxed ones have the smallest scatter.* The scatter increases of a factor ~ 2 going from R_{vir} to $2 \cdot R_{\text{vir}}$; the scatter in temperature is always larger than the scatter of the other quantities. Once that the contribution of clumpiness is removed from the datasets, post-merger clusters are the one more affected by an asymmetric distribution of the thermal gas, due to the chaotic pattern induced along mergers and filamentary accretions. The amount of azimuthal scatter is found to be in line with existing observations (see Vazza et al. 2010b for a detailed discussion), even if the presence of a un-removed clumpy component in the observation should be assumed to fit the case of clus-

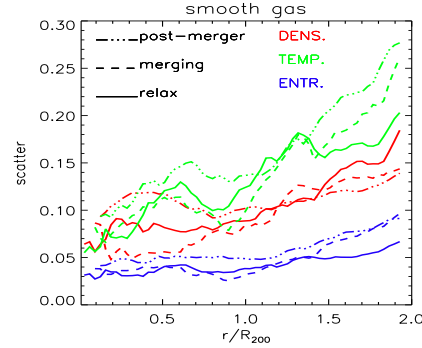


Fig. 8. Azimuthal scatter profile for our sample, after the "99 percent" filtering of the physical fields. The different colors refer to the different physical quantities, the line styles refer to the dynamical classes of the sample.

ter PKS0745-191 (George et al. 2009). These results suggest that non-gravitational processes may be not needed in simulations to model the thermodynamics of the gas in the outer cluster regions (see also Burns et al. 2010; Nagai 2011).

4. Discussion and Conclusion.

In summary, our AMR simulations with ENZO show that, for all (or most) of clusters:

- the volume and energy flux distribution of shocks in the ICM are steep and most of shocks have $M < 2$;
- the radial distribution of Mach numbers is very flat inside R_{vir} ;
- the average CR injection efficiency injection is small, $\epsilon_{\text{CR}}/\epsilon_{\text{therm}} < 0.05$;
- the kinetic energy of turbulent motions is $\sim 0.2 - 0.4$ of the total thermal energy inside R_{vir} ;
- the turbulent motions of the ICM at scales $< 30\text{kpc}$ are subsonic $v_{\text{turb}} < 0.1c_c$;
- the azimuthal scatter of the clusters profiles increases by ~ 2 from R_{vir} to $2R_{\text{vir}}$.

We find, however, the following significant dependences on the dynamical state of clusters:

- strong $M \sim 2.5 - 3.5$ shocks are found only inside the central region of clusters in $\sim 1/10$ of cases (never in relaxed clusters);
- in these rare systems, the injection efficiency of CR can be quite large, $\epsilon_{\text{CR}} \sim 0.1 - 0.2 \epsilon_{\text{therm}}$;
- in post-merger system, the turbulent energy inside $R_{\text{vir}}/3$ is $E_{\text{turb}} \sim 0.25 E_{\text{therm}}$, while it is $\sim 0.1 E_{\text{therm}}$ in post-merger systems and $\sim 0.05 E_{\text{therm}}$ in relaxed ones;
- post-merger systems present a larger volume filling factor of turbulent motions compared to relaxed systems, and host enough turbulent energy to explain radio-halos within the re-acceleration scenario (see Brunetti et al. 2007);
- the azimuthal scatter in merging and post-merger clusters is larger (by a 20 – 50 percent) compared to the relaxed ones.

5. Acknowledgments

I gratefully acknowledge my advisors and collaborators, who made all these works possible: G. Brunetti, C. Gheller, M. Brüggen, R. Brunino, M. Roncarelli, S. Ettori and K. Dolag. I also thank M. Brüggen for carefully reading the paper.

I acknowledge partial support through grant ASI-INAF I/088/06/0 and PRIN INAF 2007/2008, and grant FOR1254 from Deutschen Forschungsgemeinschaft. The simulations were produced thanks to the CINECA-INAF 2008-2010 agreement.

References

Aleksić, J., Antonelli, L. A., Antoranz, P., et al. 2010, *ApJ*, 725, 1629

Bautz, M. W., Miller, E. D., Sanders, J. S., et al. 2009, *PASJ*, 61, 1117

Brunetti, G. & Lazarian, A. 2010, *MNRAS*, 1371

Brunetti, G., Setti, G., Feretti, L., & Giovannini, G. 2001, *MNRAS*, 320, 365

Brunetti, G., Venturi, T., Dallacasa, D., et al. 2007, *ApJ*, 670, L5

Burns, J. O., Skillman, S. W., & O’Shea, B. W. 2010, *ApJ*, 721, 1105

Dolag, K., Bykov, A. M., & Diaferio, A. 2008, *Space Sci. Rev.*, 134, 311

Dolag, K., Vazza, F., Brunetti, G., & Tormen, G. 2005, *MNRAS*, 364, 753

Ferrari, C., Govoni, F., Schindler, S., Bykov, A. M., & Rephaeli, Y. 2008, *Space Sci. Rev.*, 134, 93

George, M. R., Fabian, A. C., Sanders, J. S., Young, A. J., & Russell, H. R. 2009, *MNRAS*, 395, 657

Iapichino, L. & Niemeyer, J. C. 2008, *MNRAS*, 388, 1089

Kang, H. & Jones, T. W. 2007, *Astroparticle Physics*, 28, 232

Nagai, D. 2011, ArXiv e-prints

Norman, M. L. & Bryan, G. L. 1999, in *Lecture Notes in Physics*, Berlin Springer Verlag, Vol. 530, The Radio Galaxy Messier 87, ed. H.-J. Röser & K. Meisenheimer, 106–+

Norman, M. L., Bryan, G. L., Harkness, R., & Bordner, J. a. 2007, ArXiv e-prints, 705

O’Shea, B. W., Bryan, G., Bordner, J., et al. 2004, ArXiv Astrophysics e-prints

Pfrommer, C., Springel, V., Enßlin, T. A., & Jubelgas, M. 2006, *MNRAS*, 367, 113

Roncarelli, M., Ettori, S., Dolag, K., et al. 2006, *MNRAS*, 373, 1339

Ryu, D., Kang, H., Hallman, E., & Jones, T. W. 2003, *ApJ*, 593, 599

Sanders, J. S., Fabian, A. C., & Smith, R. K. 2010, *MNRAS*, 1534

Skillman, S. W., O’Shea, B. W., Hallman, E. J., Burns, J. O., & Norman, M. L. 2008, *ApJ*, 689, 1063

Vazza, F., Brunetti, G., & Gheller, C. 2009a, *MNRAS*, 395, 1333

Vazza, F., Brunetti, G., Gheller, C., & Brunino, R. 2010a, *New A.*, 15, 695

Vazza, F., Brunetti, G., Gheller, C., Brunino, R., & Brüggen, M. 2010b, ArXiv e-prints

Vazza, F., Brunetti, G., Kritsuk, A., et al. 2009b, *A&A*, 504, 33

Vazza, F., Gheller, C., & Brunetti, G. 2010c, *A&A*, 513, A32+

Vazza, F., Roncarelli, M., Ettori, S., & Dolag, K. 2010d, ArXiv e-prints

Xu, H., Li, H., Collins, D. C., Li, S., & Norman, M. L. 2009, *ApJ*, 698, L14